International Journal of Renewable Energy Technology Research
Vol. 6, No. 2, February 2017, pp. 1-23, ISSN: 2325-3924 (Online)
Available online at http://ijretr.org

Research article

Optimization of flat-plate solar collectors used in thermosyphon solar water heater

Koholé Yemeli Wenceslas* and Tchuen Ghislain

University of Dschang, IUT-FV, LISIE / L2MSP, P.O. Box 134, Bandjoun, Cameroon.

E-mail: koholeyemeliwenceslas@yahoo.fr, tchuengse@yahoo.com.

*Corresponding author

This work is licensed under a Creative Commons Attribution 4.0 International License.

Abstract

In this paper, thermodynamic optimization based on exergy concept is developed to determine the optimal combination of values for the constructional parameters. This maximizes the exergetic efficiency of three flat-plate solar collectors commonly used in thermosyphon solar water heaters (SWH). The effect of some design parameters on the performance of a flat-plate collector has also been investigated. It has been observed that, the optimal combination of values that maximizes the exergetic efficiency for the three models are the same, with a slight difference in the maximum exergetic efficiencies. After studying a more practical situation, it has been realized that, a distance of ten centimeters between the riser tubes lead to a more cost-effective solution for designers. A change in the distance between the absorber plate and the glass cover from 0.001 to 0.03 m indicates a strong influence of the distance between the absorber plate and glass cover on the heater performance. The results also show the possibility to reach higher exergy efficiency with lower absorber area and consequently lower price. **Copyright © IJRETR, all rights reserved.**

Keywords: Absorber plate, Exergy, Flat-plate, Genetic algorithm, Water heater.

International Journal of Renewable Energy Technology Research
Vol. 6, No. 2, February 2017, pp. 1-23, ISSN: 2325-3924 (Online)
Available online at http://ijretr.org

Nomenclature

A_c	collector area (m^2)
C_b	bond conductance (W/m°C)
C_p	specific heat capacity of the absorber plate (J/kg °C)
D_i	internal diameter of the tubes (m)
D_o	outer diameter of the tubes (m)
$\dot{E}_{xdest}$	destructed exergy rate (W)
$\dot{E}_{xin}$	inlet exergy rate (W)
$\dot{E}_{xin,f}$	inlet exergy carried by the working fluid (W)
$\dot{E}_{xin,rad}$	absorbed solar radiation exergy rate (W)
$\dot{E}_{xout}$	outlet exergy rate (W)
$\dot{E}_{xout,f}$	outlet exergy rate carried by the working fluid (W)
$\dot{E}_{xu}$	useful exergy rate (W)
F	fin efficiency factor
F'	collector efficiency factor
F_R	heat removal factor
g	gravitational constant (m/s^2)
G	solar radiation (W/m^2)
$h_{c,p-c}$	convection heat transfer coefficient between the absorber plate and the cover (W/m^2°C)
$h_{r,c-a}$	radiation coefficient between the cover and the sky (W/m^2°C)
$h_{r,p-c}$	radiation heat transfer coefficient between the absorber plate and the cove (W/m^2°C)
h_w	wind convection coefficient (W/m^2°C)
h_{fi}	convective heat transfer coefficient in the tube (W/m^2°C)
k_a	thermal conductivity of air layer between absorber plate and glass (W/m°C)
k_i	thermal conductivity of the insulation (W/m°C)
k_p	thermal conductivity of the absorber plate (W/m°C)
l_a	distance between absorber plate and glass cover (m)
$\dot{m}$	mass flow rate in the collector (kg/s)

N	number of glass cover
N_u	Nusselt number
P_r	Prandtl number
Q_{u}	useful energy gain (W)
R_a	Rayleigh number
T_a	ambient temperature (°C)
T_{fi}	inlet water temperature (°C)
T_{fo}	outlet water temperature (°C)
T_s	apparent sun temperature (°C)
U_b	bottom heat loss coefficient (W/ m^2°C)
U_L	overall heat loss coefficient (W/ m^2°C)
V	wind speed (m/s)
U_t	top heat loss coefficient (W/ m^2°C)
W	distance between riser tubes (m)

Greek symbols

α	absorptivity of the absorber plate
β	collector inclination angle (degrees)
β'	volumetric coefficient of expansion
δ_i	insulator thickness (m)
δ_p	absorber plate thickness (m)
ε_c	emissivity of the glass cover
ε_p	emissivity of the absorber plate
η_{en}	energetic efficiency
η_{ex}	exergetic efficiency
σ	Stefan–Boltzmann constant (W/m^2°C^4)
υ	kinematic viscosity (m^2/s)
τ	cover transmissivity

1. Introduction

Nowadays, humans are increasingly demonstrating their awareness of the risk of some of the globe's energy resources getting completely exhausted. More stringent measures are now being taken to guarantee more efficient use of energy. This include the use of rooftop photovoltaic cells, solar water heaters, solar oven, solar cookers and solar dryers. A SWH is a device which absorbs solar radiations and uses it to produce hot water. Designing a SWH involves appropriate sizing of different components based on predicted solar radiation and hot water demand [1]. The solar collector is the heart of a SWH, and its performance is strongly affected by variation of its constructional and operating parameters. Among various types of solar collectors, flat-plate type is the world's most widely used collector because of simpler technology, lower price and easier maintenance. An optimization of the flat-plate collector will have influence on improving the performance of the SWH [2]. One of the powerful methods of optimizing complex thermo-dynamical systems such as SWHs is to do an exergy analysis. Exergy analysis, derived from first and second laws of thermodynamics includes the quality of the energy transferred, as compared to energy analysis [3]. The concept of exergy can also be used to combine and compare all flows of energy according to their quantity and quality. Unlike energy, exergy is always destroyed during conversions because of the irreversible nature of energy conversion process [4]. Attempts were made by different investigators to optimized solar flat-plate collectors in order to improve their thermal performance by employing the exergy concept.

Farahat et al [5] carried out a detailed energy and exergy analysis for a typical flat-plate solar collector in other to evaluate its thermal and optical performance, exergy flows and losses as well as its exergetic efficiency. They concluded that, the optical efficiency and inlet fluid temperature has great effect on the exergetic efficiency of a flat-plate solar collector. Hedayatizadeh et al [6] presented the optimization of a double-pass/glazed v-corrugated plate solar air heater based on exergy losses. Jafarkazemi and Ahmadifard [7] presented a theoretical model for exergy and energy analysis of flat-plate solar collectors. They evaluated the proposed model experimentally and studied the effect of some parameters such as: fluid flow rate, inlet water temperature and the type of working fluid on the energy and exergy efficiency of the collector. Said et al [8] analysed experimentally the influence of Al_2O_3-water nanofluid on the energy and exergy efficiencies of a flat-plate solar collector. Their findings revealed that, nanofluids increased the thermal performance of a flat-plate collector. Khademi et al [9] employed sequential quadratic programming and genetic algorithm for the optimization of the exergy efficiency of the flat-plate solar collector. The results proved that sequential quadratic method performs optimization process with higher convergence speed but lower accuracy than genetic algorithm. Shojaeizadeh et al [10] studied the exergy efficiency of a flat-plate solar collector containing Al_2O_3–water nanofluid as base fluid. They discussed the effect of some parameters like the fluid mass flow rate, nanoparticle volume concentration, inlet fluid temperature, solar radiation, and ambient temperature on the collector exergy. Said et al [11] investigated experimentally the energy and exergy efficiencies of a flat-plate solar collector using short single wall carbon nanotubes based nanofluid suspended in water. They found that, using improved thermo-physical properties of the nanofluid, the maximum energy and exergy efficiencies of flat-plate collector was raised up to 95.12% and 26.25% compared to water which was 42.07% and 8.77%, respectively. Badescu [12] presented optimal operation strategies for exergy gain maximization in open loop thermal solar energy collection systems. They used the water mass flow rate in the collectors as the control parameter, and found that the optimum mass flow rate increases near sunrise and sunset and by increasing the fluid inlet temperature. The results also show that during warm season, the optimum mass flow rate is well correlated with the global solar radiation. Bahrehman et al [13] used energy and exergy analysis, to analyse the effect of some parameters such as depth, length, fin shape, and Reynolds number on a single and two-glass cover solar air collector systems with forced convection flow. Golneshan and Nemati [14] derived the exergetic efficiency of unglazed transpired collector. Based on this efficiency, they optimized different cases of such a heater and proposed a simple but useful correlation to predict the optimum working temperature. Said et al [15] analysed the expanded exergy, entropy generation, the exergy destruction and the pressure drop for flat-plate solar collector operating with single wall carbon nanotubes based nanofluids as an absorbing medium. Their results shows that, the single wall carbon nanotubes nanofluid reduced the entropy generation by 4.34% and enhance the heat transfer coefficient by 15.33% compared to water as an absorbing fluid. Benli [16] compared five types of solar collectors based on the first and second law of thermodynamics. They determined the collector efficiencies, friction coefficient and exergy loss and concluded that, the heat transfer coefficient and pressure drop increase with shape of absorbers surface. Bayrak et al [17] used the first and second law of thermodynamic to analyse the performance of porous baffles inserted in solar air heaters.

To the best knowledge of the authors, a considerable improvement in the collector's performance is obtained by applying the exergetic analysis to a flat-plate collector and this help designers to achieve an optimum design and gives direction to decrease exergy losses. But yet, no study has been made employing the energetic and exergetic analysis on liquid flat-plate solar collector presented in fig. 1 below, used in thermosyphon SWH, in order to optimize its performance with respect to the geometrical design parameters.

Hence, the main objective of this paper is to derive the right optimal combination of values for the geometrical design parameters that will maximize the exergetic efficiency for three selected flat-plate collectors; and to present the effect of the distance between the absorber plate and the glass cover on the performance of the collectors.

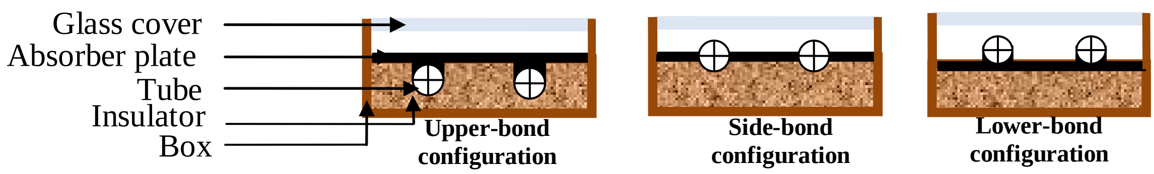

Fig .1. Various types of liquid flat-plate solar collector

2. Theoretical analysis of the Flat-plate Collector

2.1. Energetic analysis

The heat energy gain by the working from the collector absorber plate is given by [18]

$$Q_u = \dot{m} C_p \left(T_{fo} - T_{fi} \right) \tag{1}$$

Since the above equation is not helpful in the study of the effects of some constructional parameters on the performance of a collector, the Hottel-Whiller [19] equation for the useful heat gain from the solar collector, that provide the opportunity of observing the effects of some design parameters including heat loss coefficient and optical efficiency of the collector on the thermal efficiency given by the correlation below is used.

$$Qu = A_c F_R \left(G\tau\alpha - U_L \left(T_{fi} - T_a \right) \right) = A_c \left(G\tau\alpha - U_L \left(T_p - T_a \right) \right). \tag{2}$$

Where the collector heat removal factor $\left(F_R \right)$ is defined as:

$$F_R = \frac{\dot{m} C_p}{U_L A_c} \left[1 - \exp\left\{ \frac{F' U_L A_c}{\dot{m} C_p} \right\} \right]. \tag{3}$$

In (3), F' is the collector efficiency factor. For the three types of absorber configurations considered, the collector efficiencies factor, are given by the following correlations [20]:

In the case of tubes bonded below,

$$F' = \frac{1/U_L}{W \left[\frac{1}{\pi D_i h_{fi}} + \frac{1}{C_b} + \frac{1}{U_L \left[D_o + \left(W - D_o \right) F \right]} \right]}. \tag{4}$$

In the case of tubes bonded above,

$$F' = \frac{1}{\frac{W U_L}{\pi D_i h_{fi}} + \frac{1}{\frac{D_o}{W} + \frac{1}{\frac{W U_L}{C_b} + \frac{W}{\left(W - D_O \right) F}}}}. \tag{5}$$

In the case of tubes in line with the absorber plate,

$$F' = \frac{1/U_L}{W \left[\frac{1}{\pi D_i h_{fi}} + \frac{1}{U_L \left[D_o + \left(W - D_o \right) F \right]} \right]}. \tag{6}$$

The convective heat transfer coefficient in tubes h_{fi}, in the previous equations is deduced from the principles of thermal heat transfer and according to the nature of flow of the working fluid, laminar or turbulent, according to the internal diameter of the tubes and the fluid flow rate. The fin efficiency factor in (4), (5) and (6) is given by:

$$F = \frac{\tanh \left[\sqrt{\frac{U_L}{k_p \delta_p}} \frac{\left(W - D_o \right)}{2} \right]}{\sqrt{\frac{U_L}{k_p \delta_p}} \frac{\left(W - D_o \right)}{2}}. \tag{7}$$

The fin efficiency factor is a function of the overall heat loss coefficient $\left(U_L \right)$ which is given by the following equation: (It is assumed the edge loss coefficient to be negligible)

$$U_L = U_t + U_b. \tag{8}$$

For a single-glass-cover system, U_t, which is the top heat loss coefficient, is calculated with the following correlation:

$$U_t = \left(\frac{1}{h_{c,p-c} + h_{r,p-c}} + \frac{1}{h_w + h_{r,c-a}} \right)^{-1}. \tag{9}$$

For tilt angles up to 60°, the heat transfer coefficient, $h_{c;p-c}$, is given by Hollands *et al* [21] for collector inclination angle (β) in degrees:

$$Nu = \frac{h_{c,p-c} l_a}{k_a} = 1 + 1.44 \left[1 - \frac{1708}{Ra\cos(\beta)} \right]^{+} \left[1 - \frac{1708 \left[\sin(1.8\beta) \right]^{1.6}}{Ra\cos(\beta)} \right] + \left[\left(\frac{Ra\cos(\beta)}{5830} \right)^{\frac{1}{3}} - 1 \right]^{+}; \tag{10}$$

where the meaning of the + exponent is that only positive values of the terms in the square brackets are to be used (that is, use zero if the term is negative). The Rayleigh value, Ra, is given by:

$$Ra = \frac{g\beta' \Pr l_a^3}{\nu^2} \left(T_p - T_c \right). \tag{11}$$

In (9), $h_{r,p-c}$ and $h_{r,c-a}$ are the radiation heat transfer coefficient from the absorber plate to the glass cover and from the glass cover to the air respectively.

$$h_{r,p-c} = \frac{\sigma \left(T_p^2 + T_c^2 \right) \left(T_p - T_c \right)}{\frac{1}{\varepsilon_p} + \frac{1}{\varepsilon_c} - 1} \tag{12}$$

$$h_{r,c-a} = \varepsilon_c \sigma \left(T_c^2 + T_{sky}^2 \right) \left(T_c + T_{sky} \right) \tag{13}$$

where T_{sky} is the sky temperature given below as in [20]:

$$T_{sky} = 0.0552 T_a^{1.5}. \tag{14}$$

The convection heat transfer coefficient between the transparent cover and the air above, h_w, is given as

$$h_w = 5.7 + 3.8V. \tag{15}$$

Since the air properties are functions of the operating temperature, in the previous equations, solutions by iterations are required for the determination of the top heat loss coefficient. Due to the fact that, the iterations required are time consuming and tedious, straightforward determination of the top heat loss coefficient is given by the following empirical equation [22]

International Journal of Renewable Energy Technology Research
Vol. 6, No. 2, February 2017, pp. 1-23, ISSN: 2325-3924 (Online)
Available online at http://ijretr.org

$$U_t = \frac{1}{\dfrac{N}{\dfrac{C}{T_p}\left(\dfrac{T_p - T_a}{N+f}\right)^e} + \dfrac{1}{h_w}} + \frac{\sigma\left(T_p^2 + T_a^2\right)\left(T_p + T_a\right)}{\dfrac{1}{\varepsilon_p + 0.00591Nh_w} + \dfrac{2N + f - 1 + 0.133\varepsilon_p}{\varepsilon_c} - N}. \quad (16)$$

The terms f, e, C, and h_w will be calculated using,

$$f = \left(1 + 0.089h_w - 0.1166h_w\varepsilon_p\right)\left(1 + 0.07866N\right), \quad (17)$$

$$e = 0.43\left(1 - \frac{100}{T_p}\right), \quad (18)$$

$$C = 520\left(1 - 0.000051\beta^2\right), \begin{cases} 0 < \beta < 70^\circ \\ \beta = 70^\circ \ \ if \ \ \beta \geq 70^\circ \end{cases}. \quad (19)$$

In (8), the bottom loss coefficient U_b can be calculated from the following equation:

$$U_b = \frac{k_i}{\delta_i}. \quad (20)$$

In order to determine the various heat transfer coefficients at main surfaces of the flat-plate solar collector and to evaluate the overall collector heat loss coefficient the absorber temperature should be identified from the fluid inlet temperature as given in [20]

$$T_p = T_{fi} + \frac{Q_u}{A_c F_R U_L}\left(1 - F_R\right). \quad (21)$$

The mean fluid temperature T_{fm} necessary for the determination of the convective heat transfer coefficient h_{fi} for the working fluid in the absorber tubes can be determined from the inlet fluid temperature as given in [20]

$$T_{fm} = T_{fi} + \frac{Q_u}{A_c F_R U_L}\left(1 - \frac{F_R}{F'}\right). \quad (22)$$

The glass cover temperature is calculated following the methodology presented in [20]

$$T_c = T_p - \frac{U_t\left(T_p - T_a\right)}{h_{c,p-c} + h_{r,p-c}}. \quad (23)$$

The energetic efficiency of a solar collector is obtained by dividing (1), by the solar energy incident on the collector surface. Thus, the energy efficiency of the system can be written as:

$$\eta_{en} = \frac{\dot{m}C_p\left(T_{fo} - T_{fi}\right)}{A_c G}. \quad (24)$$

Using the well-known correlations of the working fluid temperature distribution in a flat-plate collector given below (25), the energetic efficiency of the flat-plate collector can be re-arranged as in (26).

$$T_{fo} = T_a + \frac{G\tau\alpha}{U_L} + \left(T_{fi} - T_a - \frac{G\tau\alpha}{U_L}\right)\exp\left(-\frac{U_L A_c F'}{\dot{m}C_p}\right) \tag{25}$$

$$\eta_{en} = \frac{\dot{m}C_p\left[\left(T_{fi} - T_a - \frac{G\tau\alpha}{U_L}\right)\left(\exp\left(-\frac{U_L A_c F'}{\dot{m}C_p}\right) - 1\right)\right]}{A_c G} \tag{26}$$

2.2. Exergetic analysis

Exergy is the maximum amount of work which can be produced by a system as it comes to equilibrium with a reference environment [23]. In order to evaluate the thermal performance of the flat-plate solar collector, the exergy equilibrium equation presented in [7] is used:

$$\sum \dot{E}x_{in} - \sum \dot{E}x_{out} = \sum \dot{E}x_{dest}\,, \tag{27}$$

where $\dot{E}x_{in}$ is the inlet exergy rate, $\dot{E}x_{out}$ the outlet exergy rate, and $\dot{E}x_{dest}$ the destructed exergy rate.

The inlet exergy rate is made of two main parts: the inlet exergy carried by the working fluid and the absorbed solar radiation exergy rate.

The first part is given as in [24]:

$$\dot{E}x_{in,f} = \dot{m}C_p\left(T_{fi} - T_a - T_a \ln\left(\frac{T_{fi}}{T_a}\right)\right). \tag{28}$$

The second part is calculated using either of the following equations presented by Spanner [25], Petela [26], and Jeter [27] respectively, that is:

$$\dot{E}x_{in,rad} = G\tau\alpha A_c\left[1 - \frac{4T_a}{3T_s}\right], \tag{29}$$

$$\dot{E}x_{in,rad} = G\tau\alpha A_c\left[1 + \frac{1}{3}\left(\frac{T_a}{T_s}\right)^4 - \frac{4T_a}{3T_s}\right], \tag{30}$$

$$\dot{E}x_{in,rad} = G\tau\alpha A_c\left[1 - \frac{T_a}{T_s}\right]; \tag{31}$$

where T_s is the solar radiation temperature and taken to be 6000 K. The differences in the results coming out from these three calculation methods are less than 2% [28]. The Jeter expression is used in our calculation.

The outlet exergy rate is made up only of the exergy rate of the outlet fluid given by [24]:

$$\dot{E}x_{out,f} = \dot{m}C_p\left(T_{fo} - T_a - T_a \ln\left(\frac{T_{fo}}{T_a}\right)\right). \tag{32}$$

The useful exergy gain is obtained by subtracting (28) from (32);

$$\dot{E}x_u = \dot{m}C_p\left[\left(T_{fo}-T_{fi}\right)-T_a\ln\left(\frac{T_{fo}}{T_{fi}}\right)\right]. \quad (33)$$

The destructed exergy rate which is generated due to the temperature difference in the solar flat-plate collector includes three terms:

The first term is the destructed exergy which resulted from the temperature difference between the sun and the absorber plate temperature [29]:

$$\dot{E}x_{dest,s-p} = \tau\alpha G A_c T_a\left(\frac{1}{T_p}-\frac{1}{T_s}\right). \quad (34)$$

The second part is the destructed exergy which resulted from the heat losses from the system to the surroundings [29]:

$$\dot{E}x_{dest,leakage} = U_L A_c\left(T_p-T_a\right)\left(1-\frac{T_a}{T_p}\right). \quad (35)$$

The third part occurs during the heat transfer process from the absorber plate to the fluid and is given as in [7]:

$$\dot{E}x_{dest,p-f} = \dot{m}C_p T_a\left[\left(\ln\frac{T_{fo}}{T_{fi}}\right)-\frac{T_{fo}-T_{fi}}{T_p}\right]. \quad (36)$$

The exergetic efficiency of the solar flat-plate collector can be defined as the ratio of the useful exergy gain to the total inlet exergy by the solar radiation [30]:

$$\eta_{ex} = \frac{\dot{m}C_p\left[T_{fo}-T_{fi}-T_a\ln\left(\frac{T_{fo}}{T_{fi}}\right)\right]}{GA_c\left[1-\frac{T_a}{T_s}\right]}. \quad (37)$$

Substituting (25) in (37) the exergetic efficiency of the collector can be re-arrange as follow:

$$\eta_{ex} = \frac{\dot{m}C_p\left[\left(T_{fi}-T_a-\frac{G\tau\alpha}{U_L}\right)\left(\exp\left(-\frac{U_L A_c F'}{\dot{m}C_p}\right)-1\right)\right]-\dot{m}C_p T_a\ln\left[\frac{\exp\left(-\frac{U_L A_c F'}{\dot{m}C_p}\right)-1}{T_{fi}}\left(T_{fi}-T_a-\frac{G\tau\alpha}{U_L}\right)+1\right]}{GA_c\left[1-\frac{T_a}{T_s}\right]}$$

(38)

As can be seen from (38), the exergetic efficiency of flat-plate collectors is a function of many design parameters, such as: the distance between the riser tubes, the internal and outer diameters of the riser tubes, the absorber plate thickness, the insulator thickness, the collector area and the collector tilt angle. The exergetic efficiency given by (38) is used as the objective function of the optimization algorithm. The genetic algorithm is used as the optimization algorithm, which helps to obtain the various geometric parameters that maximize the exergetic efficiency.

2.3. Genetic Algorithm

The genetic algorithm is an optimization and search technique based on the principles of genetics and natural selection introduced by John Holland [31]. A genetic algorithm allows a population composed of many individuals to evolve under specified selection rules to a state that maximizes the "fitness". In general, the fittest individuals of any population tend to reproduce and survive to the next generation, thus improving successive generations. However, inferior individuals can by chance, survive and also reproduce. At each step, the genetic algorithm selects individuals at random from the current population to be parents and uses them to produce the children for the next generation. Over successive generations, the population evolves toward an optimal solution [32]. A complete methodology of genetic algorithm is presented in many books, such as the book of Goldberg [33], Holland [31] and Davis [34]. The superiority of genetic algorithm is its suitability in solving nonlinear and complex problems [9].

3. Analysis

In order to construct a solar water heater with locally manufactured materials, which will be cost-effective and affordable, the various constructional parameters used as the constraints in the optimization problem has been set as shown below. The objective function of the optimization problem is as follow:

$$Objective\ \ function = \eta_{ex}. \tag{38}$$

The optimization problem can therefore be formulated as follow:

$$\begin{cases} \max\ Objective\ function = (38) \\ 0.03 \le W \le 0.2\, m, \\ 0.9 \le A_c \le 2\, m^2, \\ 0.005 \le D_i \le 0.011\, m, \\ 0.012 \le D_o \le 0.022\, m, \\ 0.05 \le \delta_i \le 0.1\, m, \\ 0.001 \le \delta_p \le 0.002\, m, \\ 30 \le \beta \le 60^\circ. \end{cases}$$

Where W, A_c, D_i, D_o, δ_i, δ_p and β are the constructional parameters of the optimization problem. Water is used as the working fluid. The considered environmental, the design conditions of the flat-plate solar collector and the constant parameters for the optimization procedure are given in table 1.

Table 1: Environmental and constant parameters used in the exergetic optimization [35]

Parameters	Values
Transmittance of glass cover, τ_c	0.88
Thermal conductivity of absorber plate, k_p	400 W/m °C
Apparent sun temperature, T_s	6000 K
Fluid specific heat, C_f	4182 J/kg °C
Number of glass cover	1
Wind speed, V	2.5 m/s
Solar radiation, G	500 W/m^2
Mass flow rate, $\dot{m}$	0.002 kg /s
Ambient temperature, T_a	22 °C
Emissivity of absorber, ε_c	0.17
Absorber plate absorptivity, α_p	0.95
Thermal conductivity of insulation, k_i	0.038 W/m °C

4. Results and Discussion

The genetic algorithm program developed consist of a population size of 375, a mutation rate of 0.01, a selection rate of 0.95 and the chromosomes type is continuous. In this work the genetic algorithm was finished when the optimum solutions were reached. Fig.2. shows the convergence diagram of the optimization procedure. As it is seen on the figure, the genetic algorithm was stopped after best fitness remained unchanged for a thousand generation.

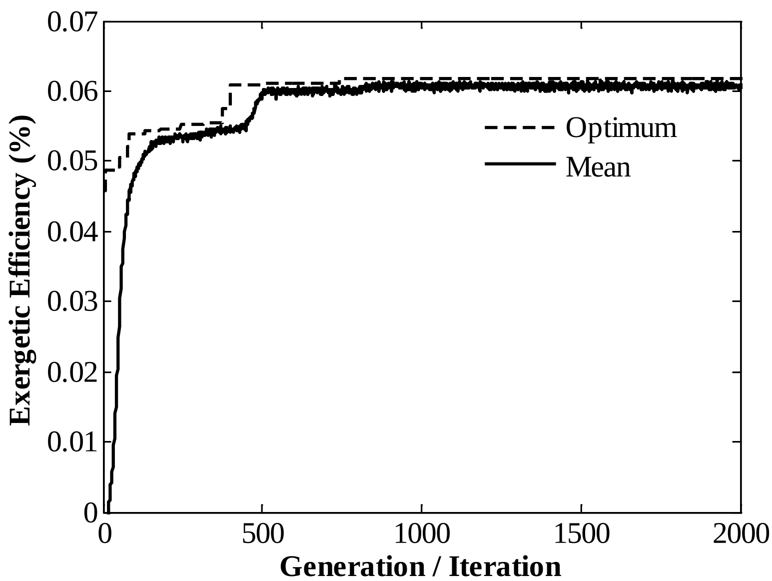

Fig.2. Convergence diagram for the optimization procedure

International Journal of Renewable Energy Technology Research
Vol. 6, No. 2, February 2017, pp. 1-23, ISSN: 2325-3924 (Online)
Available online at http://ijretr.org

The calculated value for the exergetic efficiency and the optimal combination of values for the parameters that maximizes the exergetic efficiency are presented in table 2 for the three types of flat-plate collectors.

Table 2. Results of the optimization process and maximum exergy efficiencies obtained

	W (m)	A_c (m^2)	D_i (m)	D_o (m)	δ_i (m)	δ_p (m)	β (degree)	η_{ex} (%)
Lower bond	0.03	0.9	0.011	0.012	0.05	0.001	30	6.2105
Side bond	0.03	0.9	0.011	0.012	0.05	0.001	30	6.2061
Upper bond	0.03	0.9	0.011	0.012	0.05	0.001	30	6.2023

According to the results shown in table 2, the absorber plate area, the outer diameter of the riser tubes, the distance between the riser tubes, the absorber plate thickness, the insulation thickness and collector inclination angle remain at their minimum values, while the internal diameter of the riser tubes remains at it maximum value, determined by the constrains. The figures below are obtained by varying one of the above geometrical parameters and keeping the other parameters constant.

Fig.3. shows the behavior of the exergetic efficiencies as a function of the distance between riser tubes for the three models. By varying the distance between the riser tubes in the limiting domain determined by the constraints and keeping the other parameters constant, a sensible decrease of the exergetic efficiencies from 6.2 to 5.4 % is observed.

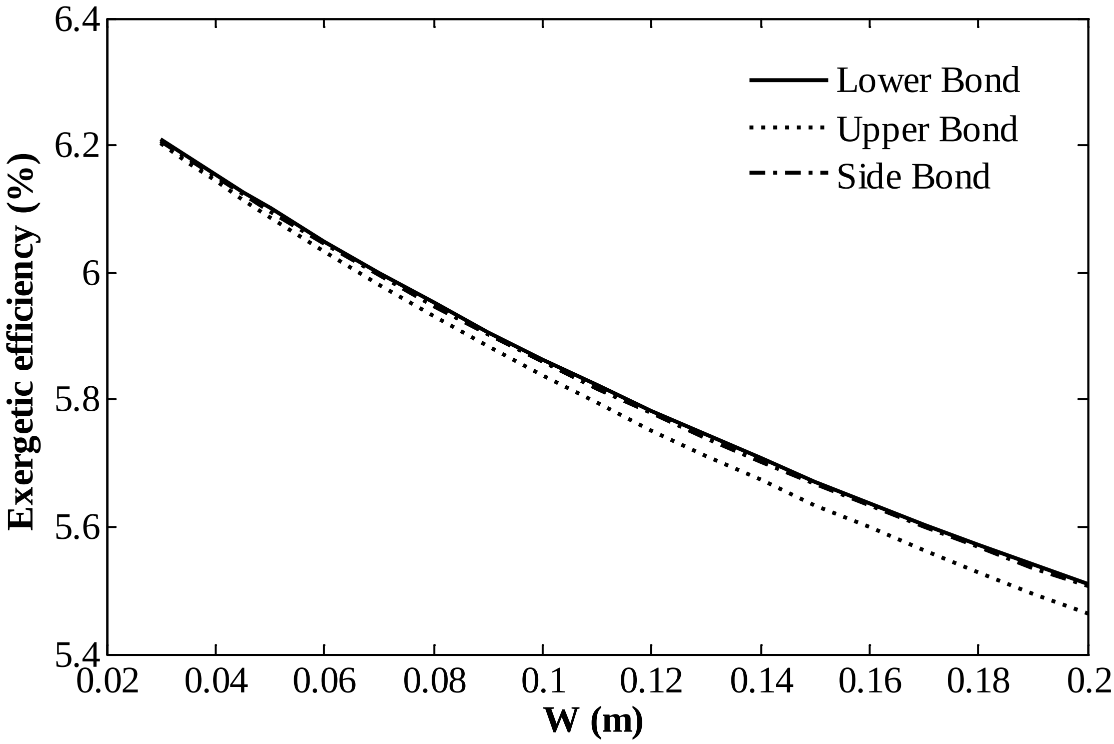

Fig. 3. The variations of the exergetic efficiencies versus the distance between riser tubes for the three models.

Fig.4. shows the variation of the exergetic efficiencies with respect to the absorber plate area for the three models. This figure reveals that, there is just a slight difference between the global maximum exergy

efficiencies obtained with the three models. For example for and area of 1.2 m^2 the maximum exergy efficiencies are 5.1680 %, 5.1644 % and 5.1631 % for the lower-bond, side-bond and upper-bond configurations respectively. Keeping the other parameters constant and varying the absorber plate area in the limiting domain, it is observed that the exergetic efficiencies start at the maximum values obtained by the optimization procedure and decrease as the absorber plate area increases. It is important to note here that, the variations of the exergetic efficiencies versus the insulator thickness and that of the exergetic efficiencies versus the collector inclination angle for the three models have the same trends as that of the exergetic efficiencies versus the absorber plate area.

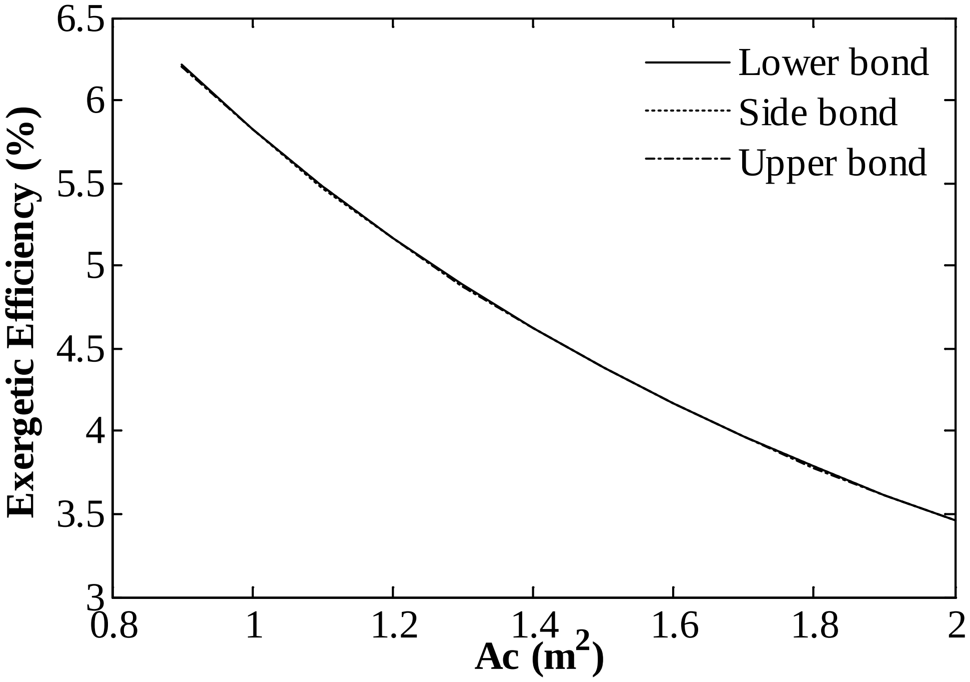

Fig. 4. The variations of the exergetic efficiencies versus the absorber plate area for the three models.

Fig. 5 shows the variations of the exergetic efficiencies with respect to the internal diameter of the riser tubes for the three models. By increasing the internal diameter of the riser tubes from 0.005 to 0.011 m with the other parameters constant, it is observed that the exergetic efficiencies increase slightly until it attains the global maximum value for a diameter of 0.011 m. Fig. 6 and 7 illustrate the variations of the exergetic efficiencies versus the outer diameter of the riser tubes and the variations of the exergetic efficiencies versus the absorber plate thickness for the three models respectively. From these figures, it can be seen that the design parameters such as the outer diameter of the riser tube and the absorber plate thickness have a little effect on the exergetic efficiencies. Thus, for a cost-effective design of collectors, decision has to be made based on cost, which increases for bigger outer diameter of the riser tubes and for bigger absorber plate thickness.

Since the distance between the consecutive riser tubes obtained above is too small, many tubes will be used and as a result, the collector will cost more. To overcome this situation, a more practical distance of ten centimetres between the riser tubes is used and this parameter is removed from the optimization procedure. The results for this situation are presented in table 3. Comparing the values obtained for this practical case with the values shown in table 2, it can be seen that the exergetic efficiencies are not affected too much and that all the other parameters presented in table 2 remain unchanged. This case however is much more cost-effective because the smaller the distance between risers tubes, the more the number of tubes and therefore the collector will be more expensive.

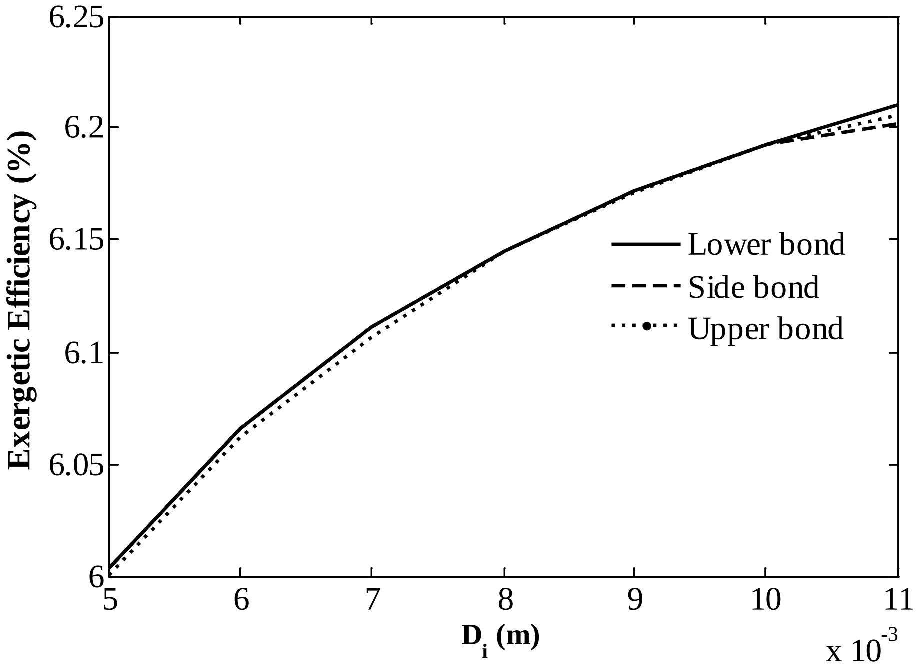

Fig. 5. The variations of the exergetic efficiencies versus the internal diameter of the riser tubes for the three models.

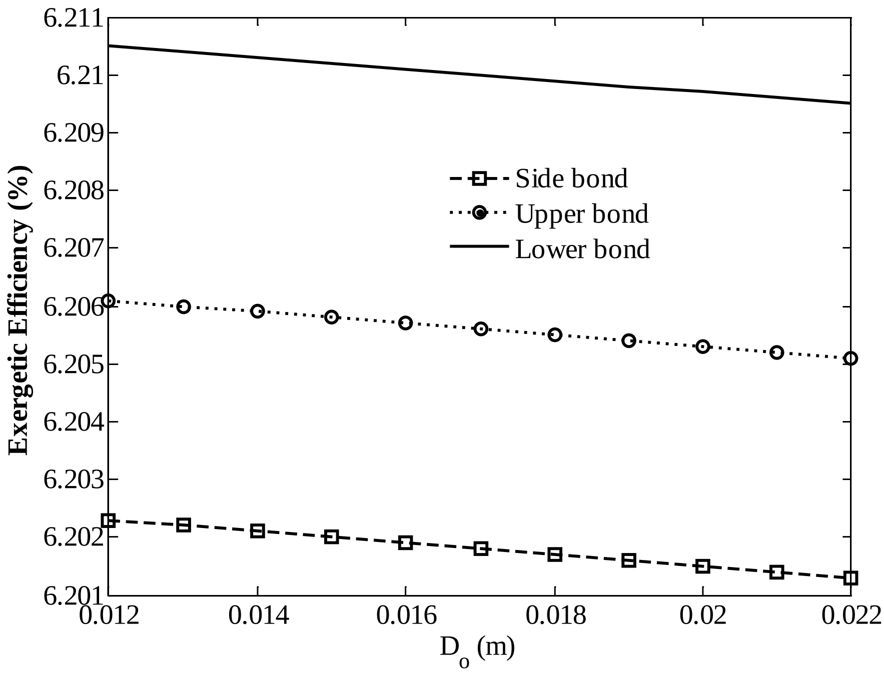

Fig. 6. The variations of the exergetic efficiencies versus the outer diameter of the riser tubes for the three models.

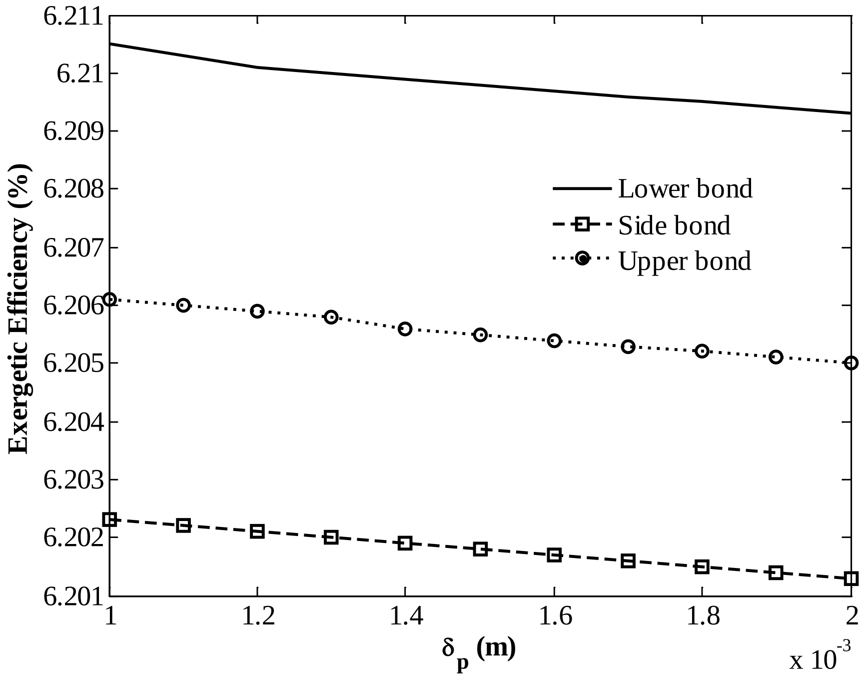

Fig. 7. The variations of the exergetic efficiencies versus the absorber plate thickness for the three models.

Table 3. Optimization results for a more practical case (distance between riser tubes = 10 cm)

	A_c (m^2)	D_i (m)	D_o (m)	δ_i (m)	δ_p (m)	β (degree)	η_{ex} (%)
Lower bond	0.9	0.011	0.012	0.05	0.001	30	5.8634
Side bond	0.9	0.011	0.012	0.05	0.001	30	5.8593
Upper bond	0.9	0.011	0.012	0.05	0.001	30	5.8379

4.1. Comparison with previous works

To validate the present results, the numerical code is first validated using design parameters considered by Khademi et al [9] as input data for the optimisation program. The maximum exergetic efficiency obtained with these parameters is found to be 7.224 %. Comparing the optimal obtained result (7.224 %.) for this case with the optimal results (7.002 %) obtained using genetic algorithm by Khademi et al [9] a deviation of 0.222 is observed. Since Khademi et al [9] did not indicate the solar flux density there used in their numerical computing, this difference can be attributed to the solar flux density consider to be 500 W/m^2 in the current study. In order to compare our results with previous published works, the experimental results of Luminosu and Fara [36] for the open circuit mode of the solar collector with serpentine ducts, the numerical simulation results of Farahat et al [5], Khademi et al [9] and Mukhopadhyay [37] are used. Table 4 compares the analysed exergetic efficiency with an experimental work [36] and the computer simulation results of [5, 9, and 37]. The global maximum points suggested by Luminosu and Fara [36] are: Ac = 3.5 m^2, η_{ex} =2.90 %. For almost the same collector, Khademi et al [9] obtained exergy efficiency = 7.002 %. The optimal exergy efficiency that was obtained in [37] for a solar collector with area Ac= 3.12 m^2 is η_{ex} =5.20 %. The calculated values for the global maximum point obtained by Farahat et al [5] are Ac = 9.14 m^2 and η_{ex} =3.89 %. Comparing the exergetic efficiencies obtained in the present study as shown in tables 2 and 3 with that obtained by Khademi et al [9] (7.0002% for an area of 3.12 m^2), Farahat et al [5] (3.898%, for an area of 9.14 m^2), Luminosu and Fara [36] (2.90 %, for an area of 3.5 m^2), and Mukhopadhyay [37] (2.13 %, for an area of 5.20 m^2), it can be concluded that, the results obtained in the present work show the possibility to reach higher exergy efficiency with lower absorber area. It is important to mention here that the exergy efficiencies presented above are weak because of the irreversibilities (exergy destructions) taking place in flat-plate solar collectors. The present numerical simulation results determines the right combination of values for the various geometrical parameters that maximizes the exergetic efficiency; and it show the possibility to reach higher exergy efficiency with lower absorber area and consequently lower price. The present results are also in good agreement with the experimental data presented in [36] because for the same input parameters, the outlet fluid temperatures are almost the same. But a significant difference in optimal values of exergy efficiency is noted between the present results and that of Luminosu and Fara [36]. This may be due to the simplifying assumption for sun's exergy flow rate they made.

Table 4. Comparison between the present numerical simulation results and experimental [36] and computer results [5, 9, and 37].

	T_{fi} (K)	G (W/m^2)	T_{fo} (k)	$\left(\Delta T = T_{fo} - T_{fi}\right)$(k)	A_c (m^2)	η_{ex} (%)
Luminosu and Fara [36]	305.15	788	351.15	46.00	3.5	2.90
Farahat et al [9]	300.00	500	358.82	58.82	9.14	3.89
Khademi et al [5]	300.00	Not found	407.68	107.68	3.12	7.002
Mukhopadhyay [37]	303.00	800	380.01	77.01	2.13	5.20
Present work	302.00	800	351.45	51.45	0.90	6.21

4.2. Parametric study

Employing the mathematical model presented above, the effect of the distance between the absorber plate and glass cover on the thermal performance of a flat-plate solar collector is examined in this section. Fig. 8 indicates that increasing the distance between the absorber plate and glass cover to approximately 0.03 m leads to a considerable increase in the absorber plate temperature. This increase in the absorber plate temperature leads to a decrease in the heat loss coefficient for any increase in the distance between the absorber plate and glass cover, and consequently to an increase in the thermal efficiency of the collector (Fig. 9).

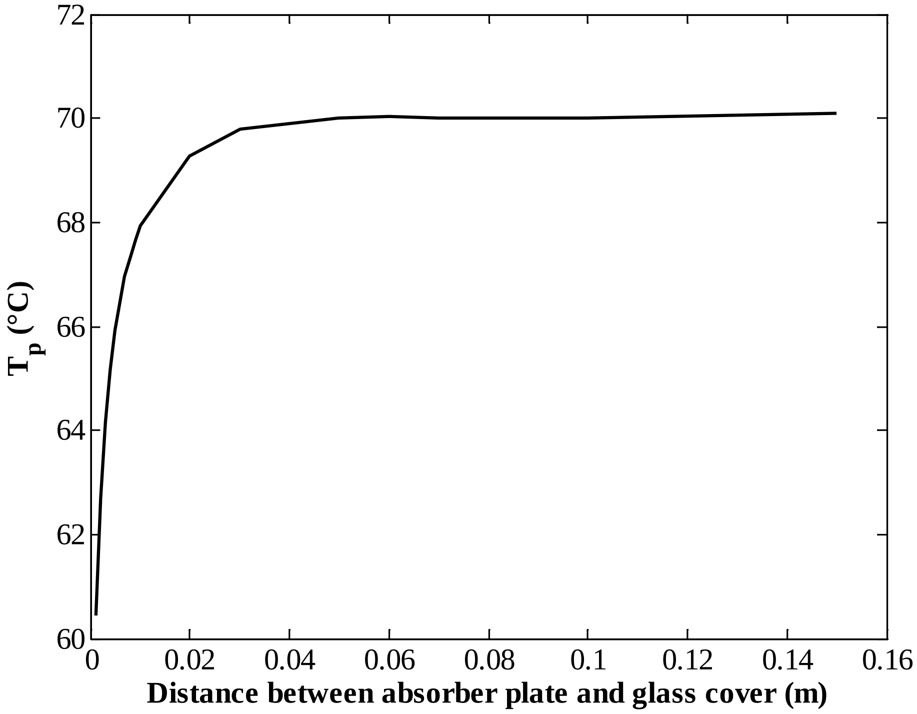

Fig.8. Variations of the absorber plate temperature versus the distance between absorber plate and glass cover.

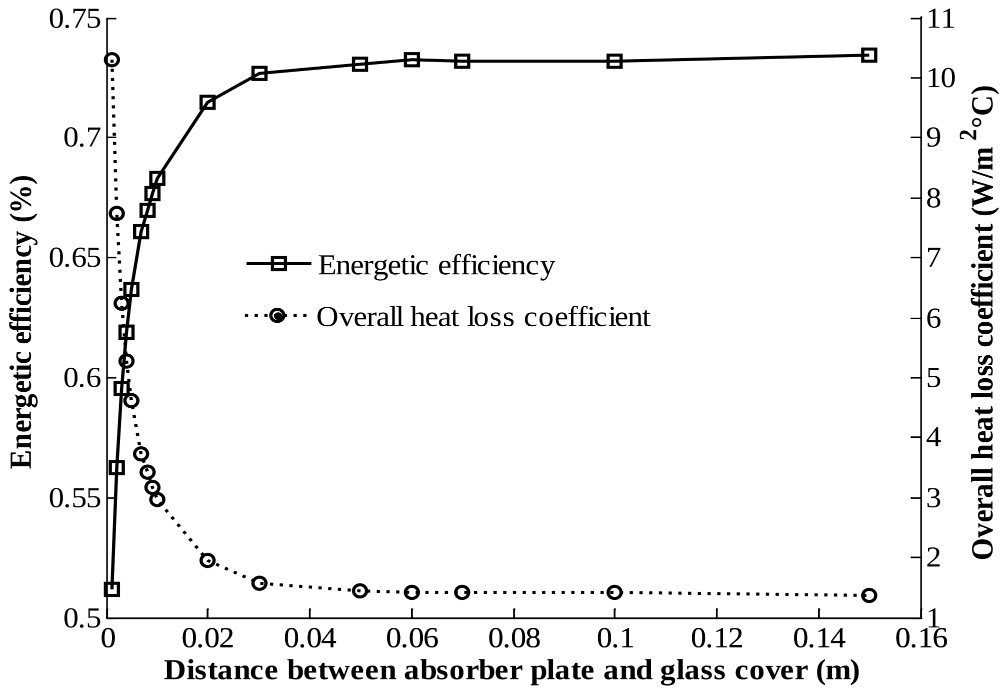

Fig.9. Variations of energetic efficiency and overall heat loss coefficient versus the distance between absorber plate and glass cover.

For a more precise and complete analysis of the exergetic efficiency of the flat-plate solar collector, exergy destruction components which are generated due to the temperature difference in the solar flat-plate collector are taken into consideration. Considering fig. 8, it is obvious that, the absorber plate temperature increases as the distance between the absorber plate and glass cover increases. As a result, the destructed exergy which is due to the temperature difference between the sun and the absorber plate temperature will decrease as illustrated in fig. 10.

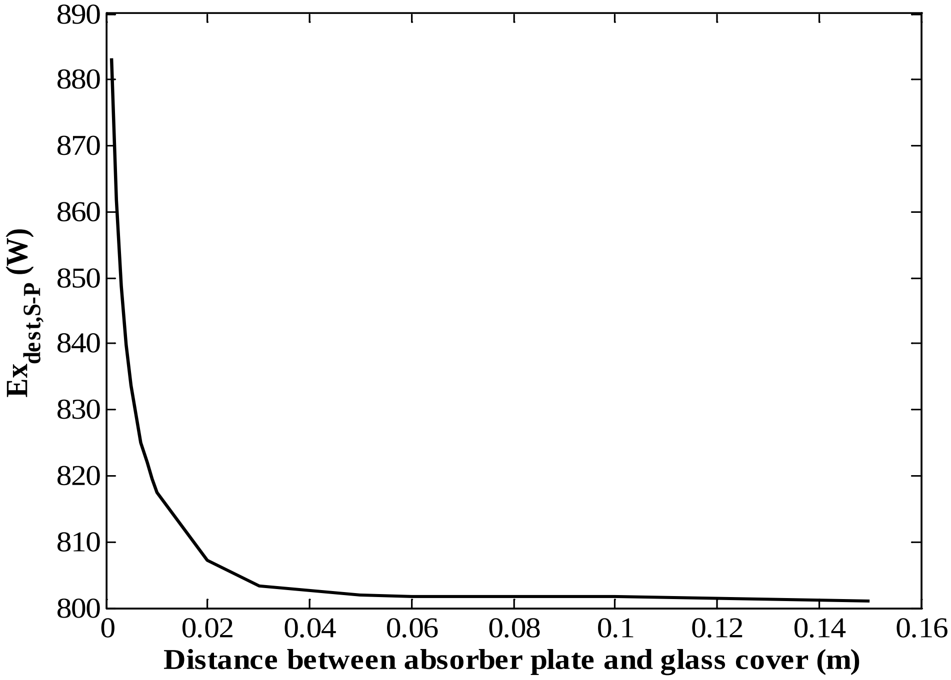

Fig.10. Variations of absorption exergy losses versus the distance between absorber plate and glass cover.

The evolution of $Ex_{dest,leakage}$ and the exergetic efficiency versus the distance between the absorber plate and glass cover is shown in fig. 11. As it has been shown in fig. 9, increasing the distance between the absorber plate and the glass cover leads to a considerable decrease in the overall heat loss coefficient (fig. 9). The decrease in the overall heat loss coefficient leads to a decrease in the exergy destruction due to collector’s heat losses as shown in fig. 11, and consequently to an increase in the exergetic efficiency of the flat-plate collector (fig. 11). Therefore, increasing the distance between the absorber plate and the glass cover leads to an increase in the exergetic efficiency of the heater. Fig. 12 show the evolution of $Ex_{dext,p-f}$ versus the distance between the absorber plate and the glass cover. Increasing the distance between the absorber plate and glass cover leads to an increase in the rate of exergy destruction in the heat transfer process from the absorber plate to the working fluid.

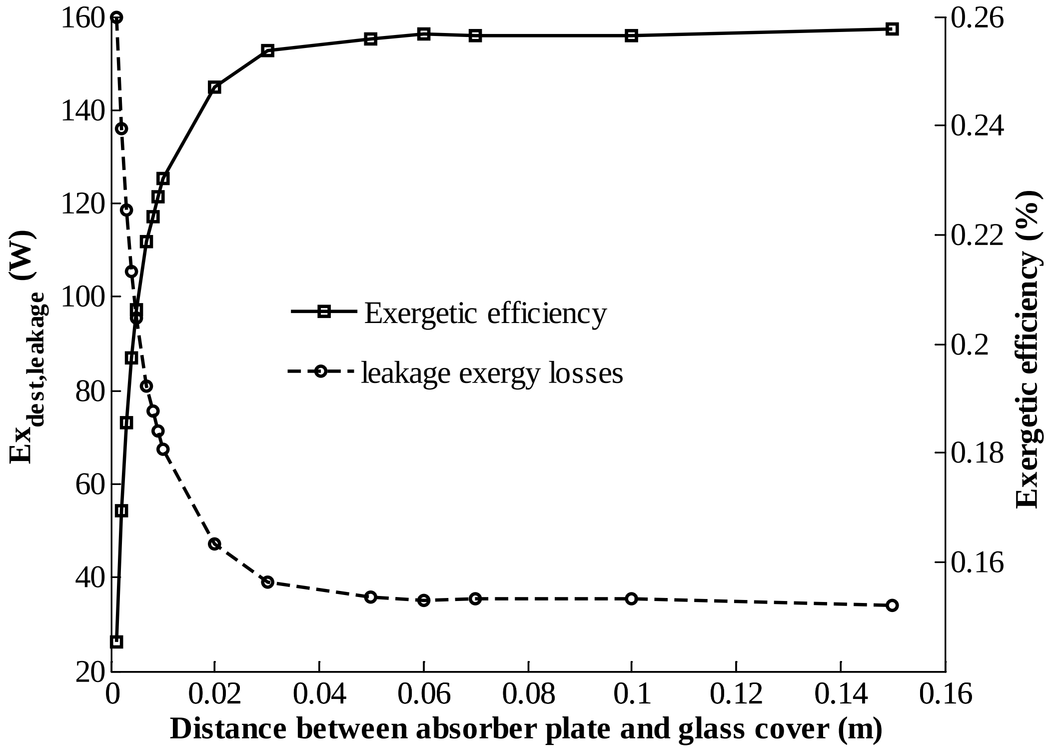

Fig.11. Variations of leakage exergy losses and exergetic efficiency versus the distance between absorber plate and glass cover

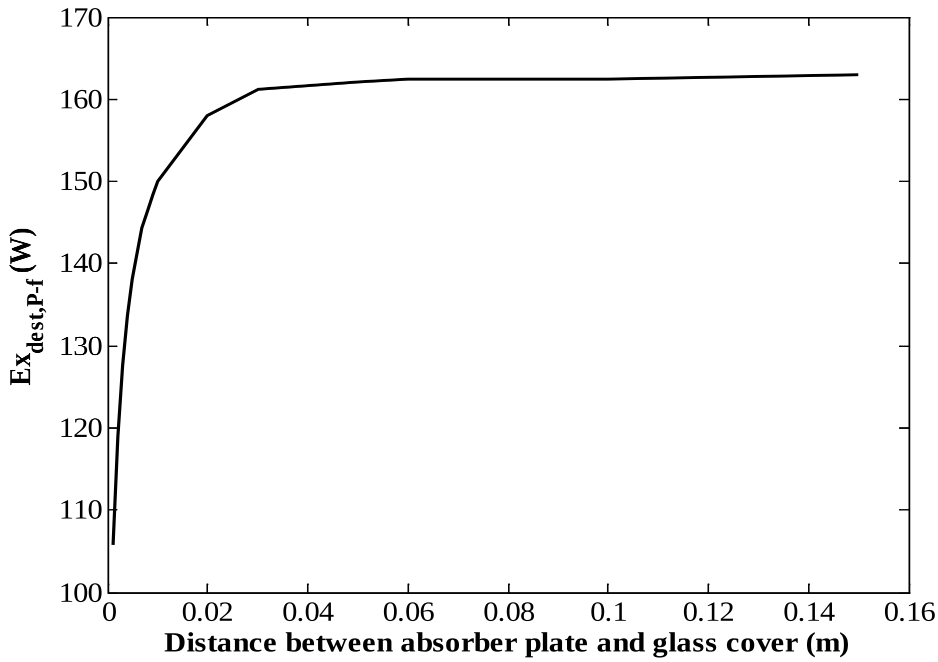

Fig.12. Variations of exergy destructing in the heat transfer process from absorber plate to working fluid versus the distance between absorber plate and glass cover.

5. Conclusion

In this paper, the exergetic optimization of three flat-plate solar collectors mostly used in thermosyphon SWH with the help of genetic algorithms is presented; and the effect of the distance between the absorber plate and the glass cover on the performance of such a heater were also investigated. A number of seven parameters linked to the dimensions of different components, were considered as the restrictions in the optimization problem and other parameters were kept constant. The optimal combination of values for the optimization parameters that maximizes the exergetic function is obtained for the three flat-plate collectors. It has been observed that, the optimal combination of values that maximizes the exergetic efficiency for the three models are the same, with a slight difference in the maximum exergetic efficiencies. After studying a more practical situation it has been realized that a distance of ten centimeters between the riser tubes lead to a more cost-effective solution for designers since the exergetic efficiency is not affected too much. It has also been observed that, the efficiencies of the collector are nearly constant for the distance between the absorber plate and glass cover greater than 0.04 m. A change in the distance between the absorber plate and the glass cover from 0.001 to 0.03 m resulted in an increase in the efficiencies of the heater, indicating the strong influence of the distance between the absorber plate and glass cover on collector efficiencies. The above findings also show the possibility to reach higher exergy efficiency with lower absorber area and consequently lower price.

References

[1] G. N. Kulkarni, S. B. Kedare and S. Bandyopadhyay, "Determination of design space and optimization of solar water heating systems." Solar Energy, vol. 81, pp. 958–968, 2007.

[2] N. Mohammadi and A. Mohammadzadeh, "Optimizing the Collector Performance of a Solar Domestic Hot Water System by the Use of Imperialist Competitive Algorithm with the Help of Exergy Concept." International Journal of Engineering and Technology Science, vol. 3, pp. 65-78, 2015.

[3] P. Velmurugan and R. Kalaivanan, "Energy and Exergy Analysis of Multi-Pass Flat Plate Solar Air Heater—an Analytical Approach," International Journal of Green Energy, vol. 12, pp. 810–820, 2015.

[4] A. vosough and S. vosough, "Different Kind of Renewable Energy and Exergy Concept," International Journal of Multidisciplinary Sciences AND Engineering, vol. 2, December 2011.

[5] S. Farahat, F. Sarhaddi and H. Ajam, "Exergetic optimization of flat plate solar collectors," Renewable Energy, vol. 34, pp. 1169–1174, 2009.

[6] M. Hedayatizadeh, F. Sarhaddi, A. Safavinejad, F. Ranjbar and H. Chaji, "Exergy loss-based efficiency optimization of a double-pass/glazed v-corrugated plate solar air heater," Energy, vol. 94, pp. 799–810, 2016.

[7] F. Jafarkazemi and E. Ahmadifard, "Energetic and exergetic evaluation of flat plate solar collectors," Renewable Energy, vol. 56, pp. 55-63, 2013.

[8] Z. Said, R. Saidur, M. A. Sabiha, A. Hepbasli and N. A. Rahim, "Energy and exergy efficiency of a flat plate solar collector using pH treated Al_2O_3 nanofluid," Journal of Cleaner Production, vol. 112, pp. 3915-3926, 2016.

[9] M. Khademi, F. Jafarkazemi, E. Ahmadifard and S. younesnejad, "Optimizing Exergy Efficiency of Flat Plate Solar Collectors Using SQP and Genetic Algorithm." Applied Mechanics and Materials, vols. 253-255, pp. 760-765, 2013.

[10] E. Shojaeizadeh, F. Veysi and A. Kamandi, "Exergy efficiency investigation and optimization of an Al_2O_3–water nanofluid based Flat-plate solar collector," Energy and Buildings, vol. 101, pp. 12–23, 2015.

[11] Z. Said, R. Saidur, M. A. Sabiha, N. A. Rahim and M. R. Anisur, "Thermo-physical properties of Single Wall Carbon Nanotubes and its effect on exergy efficiency of a flat plate solar collector," Solar Energy, vol. 115, pp. 757–769, 2015.

[12] V. Badescu, "Optimal control of flow in solar collectors for maximum exergy extraction," International Journal of Heat and Mass Transfer, vol. 50, pp. 4311–4322, 2007.

[13] D. Bahrehmand, M. Ameri and M. Gholampour, "Energy and exergy analysis of different solar air collector systems with forced convection," Renewable Energy, vol. 83, pp. 1119–1130, 2015.

[14] A. A. Golneshan and H. Nemati, "Exergy analysis of unglazed transpired solar collectors (UTCs)," Solar Energy, vol. 107, pp. 272–27, 2014.

[15] Z. Said, R. Saidur, N. A. Rahim and M. A. Alim, "Analyses of exergy efficiency and pumping power for a conventional flat plate solar collector using SWCNTs based nanofluid," Energy and Buildings, vol.78, pp. 1–9, 2014.

[16] H. Benli, "Experimentally derived efficiency and exergy analysis of a new solar air heater having different surface shapes," Renewable Energy, vol. 50, pp. 58-67, 2013.

[17] F. Bayrak, H. F. Oztop and A. Hepbasli, "Energy and exergy analyses of porous baffles inserted solar air heaters for building applications," Energy and Buildings, vol. 57, pp. 338–345, 2013.

[18] S. A. Kalogirou, "Solar Energy Engineering: Processes and Systems," New York: Academic press, Elsevier Science; 2009.

[19] H. C. Hottel and A. Whillier, "Evaluation of Flat-Plate Solar Collector Performance." Transactions of the Conference on the use of Solar Energy - The Scientific Basis, Vol. 2, Tucson, AZ, October 31–November 1, pp. 74–104, 1955.

[20] J. A. Duffie and W. A. Beckman, "Solar engineering of thermal processes," 3rd edition, J. Wiley, 2006.

[21] K. G. T. Hollands, T. E. Unny, G. D. Raithby and L. Konicek, "Free convective heat transfer across inclined air layers," Transactions of ASME, Journal of Heat Transfer, vol. 98 pp. 189-193, 1976.

[22] S. A. Klein, "Calculation of Flat-Plate Collector Loss Coefficients," Solar Energy, vol. 17 pp. 79-80, 1975.

[23] T. J. Kotas, "The exergy method of thermal plant analysis," Malabar, FL: Krieger Publish Company; 1995.

[24] A. Bejan, "Advanced Engineering Thermodynamics," Wiley Interscience: New York, NY, USA, 1988.

[25] D. C. Spanner, "Introduction to thermodynamics," London: Academic Press; 1964.

[26] R. Petela, "Energy of heat radiation," J Heat Transfer, vol. 86, pp. 187–92, 1964.

[27] S. M. Jeter, "Maximum conversion efficiency for the utilization of direct solar radiation," Solar Energy, vol. 26, pp. 231–236, 1981.

[28] T. T. Chow, G. Pei, K. F. Fong, Z. Lin, A. L. S. Chan and J. Ji, "Energy and exergy analysis of photovoltaic -thermal collector with and without glass cover," Applied Energy, vol. 86, pp. 310–316, 2009.

[29] K. K. Gupta and S. K. Saha, "Energy analysis of solar thermal collectors," Renewable Energy and Environment, pp. 283–7, 1990.

[30] N. Singh, S. C. Kaushik and R. D. Misra, "Exergetic Analysis of a Solar Thermal Power System," Renewable Energy, vol. 19, pp. 135–143, 2000.

[31] J. Holland, "Adaptation in natural and artificial systems," University of Michigan Press, 1975.

[32] G. Kumaresan, "Optimizing Design of Heat Pump Using Fuzzy Logic and Genetic Algorithm," International Journal of Engineering Research and Applications, vol. 3, pp. 1184-1189, 2013.

[33] D. E. Goldberg, "Genetic Algorithms in Search Optimization and Machine Learning, Reading," MA: AddisonWesley; 1989.

[34] L. Davis, "The handbook of genetic algorithms," Van Nostran Reingold, New York. 1991.

[35] Koholé, Y. W. and Tchuen, G. Comparative study of three thermosyphon solar water heaters made of flat-plate collectors with different absorber configurations, International Journal of Sustainable Energy, vol. 36, pp. 430–449, 2017.

[36] Luminosu, I., Fara, L. Determination of the optimal operation mode of a flat solar collector by exergetic analysis and numerical simulation. Energy, vol. 30; pp.731- 747, 2005.

[37] Mukhopadhyay, S. D. Simulation of Optimal Exergy Efficiency of Solar Flat Plate Collector. Jordan Journal of Mechanical and Industrial Engineering, vol.10, pp. 51- 65, 2016.